Asian Journal of Chemistry; Vol. 36, No. 12 (2024), 2827-2836

ASIAN JOURNAL OF CHEMISTRY

https://doi.org/10.14233/ajchem.2024.32677

Novel Pyrrolo-Pyrimidine Derivatives Bearing Amide Functionality as Potential Anticancer Agents: Synthesis and Molecular Docking Studies

PRAVEEN KUMAR BANDARU[1,*], N.S. KAMESWARA RAO[2] and P. SHYAMALA[2]

[1]Department of Chemistry, Andhra University, Visakhapatnam-530003, India
[2]Aragen Life Sciences Pvt. Ltd., Plot No 28 A, IDA, Nacharam-Mallapur Road, Nacharam, Hyderabad-500076, India

*Corresponding author: E-mail: praveenbandaruchemist@gmail.com

Received: 8 September 2024; *Accepted*: 24 October 2024; *Published online*: 30 November 2024; AJC-21823

Current investigation presents the synthesis, molecular docking and anticancer evaluation of novel pyrrolo-pyrimidine derivatives designed to target Janus kinase 1 (JAK1), Janus kinase 2 (JAK2) and cyclin-dependent kinase 4 (CDK4). The synthesis route commenced with 2-amino-4,6-dichloropyrimidine-5-carbaldehyde, proceeding through sequential steps involving intermediate formations and coupling reactions to yield a diverse array of pyrrolo-pyrimidine derivatives. Characterization using spectroscopic techniques (^{1}H NMR, ^{13}C NMR and HRMS) confirmed the chemical structures of the synthesized compounds. Molecular docking studies against JAK1, JAK2 and CDK4 demonstrated substantial binding affinities, remarkably compounds **7k**, **7l** and **7d**, which displayed promising interactions within the active sites of the proteins. Anticancer evaluation against breast cancer (MCF-7), chronic myeloid leukemia (SET-2), colorectal carcinoma (HCT-116) and HEK-293 cell lines revealed diverse cytotoxic profiles. Specifically, compounds **7k** and **7f** exhibited potent activity against breast cancer (MCF-7), **7k** and **7f** showed efficacy against chronic myeloid leukemia (SET-2) and compounds **7k** and **7l** demonstrated effectiveness against colorectal carcinoma (HCT-116). These findings underscore the potential of these pyrrolo-pyrimidine derivatives as selective and effective anticancer agents, prompting further exploration for therapeutic development.

Keywords: Pyrrolo-pyrimidine derivatives, MTT assay, Molecular docking, Anticancer activity.

INTRODUCTION

Recent data projects 9.7 million deaths and 20 million new cancer cases in 2022. In 5 years after obtaining a cancer diagnosis, an estimated 53.5 million people were still alive. During their lifetime, one in five individuals may develop cancer and one in nine men and one in twelve women will succumb to the disease. The data from the International Agency for Research on Cancer (IARC), which is part of the WHO, highlight the critical need for novel anticancer drugs [1]. Radiation therapy [2], chemotherapy [3] and surgery [4] are only a few of the treatment modalities that have advanced in recent years, but many cancers still do not respond to these methods and some even develop resistance. As such, there is a pressing need for novel treatments that can minimize side effects on healthy organs while efficiently and specifically targeting cancer cells. Researchers are exploring heterocyclic scaffolds, specifically pyrrolo[2,3-*d*]pyrimidines, in their search for novel anticancer drugs, as these scaffolds have demonstrated promising pharmacological properties. The pyrrolo[2,3-*d*]pyrimidine nucleus presents numerous benefits in the field of drug development, such as its structural variety and its capacity to participate in a wide range of molecular interactions, which are essential for biological activity. It is worth mentioning that a small number of anticancer medications, specifically ribociclib (used for breast cancer) [5,6], ruxolitinib (used for myelofibrosis) [7] and pemetrexed (used for pleural mesothelioma of non-small cell lung cancer (NSCLC)) [8], which contain pyrrolo[2,3-*d*]-pyrimidine nucleus, have shown clinical effectiveness.

This emphasizes the importance of this structure in cancer treatment. Many research groups have reported the anticancer activity of various organic compounds containing a pyrrolo-[2,3-*d*]pyrimidine nucleus. These compounds demonstrate a range of molecular mechanisms that contribute to their anticancer effects. Specifically, they inhibit Janus Kinases (JAK1, JAK2 and JAK3) [9-11], which are critical for cytokine signa-

ling and immune function. Additionally, they target cyclin-dependent kinases [12-15], essential regulators of cell cycle progression. These compounds also inhibit *c*-Met kinases [16-18], which are involved in cell growth, motility and differentiation and Bruton's tyrosine kinase (BTK) [19,20], important for B-cell development. Furthermore, they affect EGFR [21-23], a key player in cell growth and survival signaling pathways and VEGFR [24-27], which is crucial for angiogenesis and the formation of new blood vessels. By targeting these diverse pathways, pyrrolo[2,3-*d*]pyrimidine-based compounds offer promising potential for the development of new anticancer therapies. The success of ribociclib, ruxolitinib and pemetrexed (Fig. 1) in cancer treatment underscores the therapeutic potential of pyrrolo[2,3-*d*]pyrimidine-based compounds. This success serves as an incentive for additional investigation of this scaffold in order to develop innovative anticancer drugs with enhanced safety and efficacy profiles.

In this study, we present the synthesis, characterization and evaluation of a series of novel pyrrolo[2,3-*d*]pyrimidine based compounds bearing amide functionality. Their anticancer activity against different cancer cell lines is being thoroughly investigated in the present study to provide light on their development. Additionally, molecular docking studies are conducted to provide insights into the binding modes and interactions of these compounds with key biological targets implicated in cancer progression. By employing a multidisciplinary approach that integrates synthetic chemistry, biological assays and computational modelling, this research seeks to contribute to the advancement of anticancer drug discovery. The findings presented herein not only expand the chemical diversity of pyrrolo[2,3-*d*]-pyrimidine analogues but also offer valuable insights into their potential as therapeutic agents for combating cancer.

EXPERIMENTAL

No further purification procedures were employed after employing the laboratory grade chemicals and solvents that were purchased from Sigma-Aldrich, India. Merck-precoated aluminium TLC plates coated with silica gel 60 F_{254} were employed for the purpose of reaction monitoring. The melting points were determined using Remi electronic melting point apparatus and are uncorrected. The chemical shift values in ppm, were relative to the internal standard, tetramethyl silane and were taken using a VARIAN-INOVA (500 MHz) instrument to acquire the ^{1}H and ^{13}C NMR spectra. The HRMS spectra were obtained by utilizing a Waters Xevo Q-Tof Mass spectrometer in their collection. The cell lines (ATCC) for the anticancer activity were obtained from HiMedia Laboratories Pvt. Ltd., India.

Synthesis of methyl(2-amino-6-chloro-5-formyl-pyrimidin-4-yl)glycinate (3): To a 50 mL round-bottom flask, 2-amino-4,6-dichloropyrimidine-5-carbaldehyde (**1**, 2.0 mmol) and 10 mL of ethanol were mixed. Triethylamine (2.2 mmol) and methyl glycinate (**2**, 2.0 mmol) were sequentially added while stirring. The mixture was stirred at room temperature for 3 h. The precipitate was collected by vacuum filtration, washed with water (3 × 5 mL) and 1 mL of methanol, then dried. The dried solid was dissolved in hot 2-propanol, cooled slowly to room temperature and then cooled in an ice bath. The recrystallized product was collected by vacuum filtration, washed with cold 2-propanol and dried under reduced pressure, yielding compound **3** [28].

Synthesis of methyl 2-amino-4-chloro-7*H*-pyrrolo[2,3-*d*]-pyrimidine-6-carboxylate (4): A suspension of compound **3** (1.1 mmol) in ethanol (10 mL) and triethylamine (1.1 mmol) was refluxed for 12 h. After cooling to room temperature, the precipitate was collected by filtration, washed with water (3 × 5 mL) and methanol (1 mL) and then dried. The crude product was recrystallized from a DMF-water mixture to yield methyl 2-amino-4-chloro-7*H*-pyrrolo[2,3-*d*]pyrimidine-6-carboxylate (**4**).

Synthesis of 2-amino-4-chloro-7*H*-pyrrolo[2,3-*d*]-pyrimidine-6-carbaldehyde (5): Compound **4** (30 mmol) was dissolved in hexane (25 mL) and cooled to -78 ºC. In a separate flask, diisobutylaluminum hydride (DIBAL-H, 1.0 M in hexane, 31 mmol) was also cooled to -78 ºC. The DIBAL-H solution was transferred *via* cannula over 20-25 min and stirred at -78 ºC for 1 h. The reaction mixture was quenched by adding methanol (10 mL) and stirred at -78 ºC for 15 min. The cold solution was then transferred to a 1 L flask containing saturated Rochelle salt solution (60 mL) and stirred for 3.5 h. The aqueous phase was separated and further extracted with hexane (20 mL). The combined organic layers were washed with brine (20 mL), dried over $MgSO_4$, filtered and concentrated to yield 2-amino-4-chloro-7*H*-pyrrolo[2,3-*d*]-pyrimidine-6-carbaldehyde (**5**) [29,30].

Synthesis of 4-chloro-6-methyl-7*H*-pyrrolo[2,3-*d*]-pyrimidin-2-amine (6): A mixture of compound **5** (7.5 mmol) and hydrazine hydrate (37 mmol) was heated to 80 ºC. To the resulting suspension, KOH (5 mmol) was added and the mixture was stirred at 80 ºC. Three additional portions of KOH (5 mmol each) were added at 20 min intervals and the temperature was

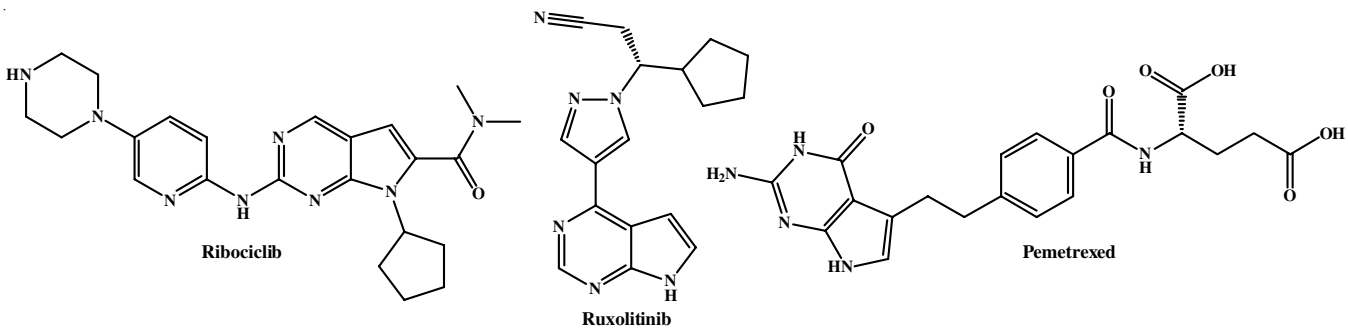

Fig. 1. Anticancer drugs containing pyrrolo[2,3-*d*]pyrimidine pharmacophore

then raised to 110 ºC. After stirring overnight, the reaction mixture was acidified with cold concentrated aqueous HCl. The product was extracted with MTBE (2 × 15 mL). The combined organic layers were washed with water (2 × 15 mL) and brine (25 mL), then concentrated *in vacuo* until solids began to crystallize. The solids were filtered to yield 4-chloro-6-methyl-7*H*-pyrrolo[2,3-*d*]pyrimidin-2-amine (**6**).

Synthesis of pyrrolo-pyrimidine derivatives (7a-r): The carboxylic acid **(a-r)** (1.0 mmol, 1.0 equiv.) was dissolved in dry DCM (10 mL/1 mmol of carboxylic acid) in a reaction flask equipped with a magnetic stir bar. To this solution, N,N′-dicyclohexylcarbodiimide (DCC) (1.2 equiv.) was added while stirring in an ice bath and the mixture was stirred for 15-30 min. Subsequently, 4-dimethylaminopyridine (DMAP) (0.1 equiv.) was added to the reaction mixture. The primary amine **6** (1.0 equiv) was then added slowly while maintaining stirring in the ice bath. The reaction mixture was allowed to gradually warm to room temperature and stirred for 18 h, with the progress monitored by thin-layer chromatography (TLC). Upon completion, the reaction was quenched by adding water (10 mL) and the mixture was extracted with DCM (3 × 20 mL). The combined organic layers were washed with saturated Na_2CO_3 solution (2 × 20 mL) and brine (20 mL) and then dried over anhydrous $MgSO_4$ (**Scheme-I**). After filtration, the solvent was removed under reduced pressure using a rotary evaporator. The crude product was purified by column chromatography on silica gel using hexane:ethyl acetate (8:2 v/v) as eluent.

***N*-(4-Chloro-6-methyl-7*H*-pyrrolo[2,3-*d*]pyrimidin-2-yl)benzamide (7a):** Pale yellow solid, yield: 78%, m.p.: 244-245 ºC; ^{1}H NMR (500 MHz, $CDCl_3$-d_6) δ ppm: 10.73-10.69 (s, 1H), 9.67-9.63 (s, 1H), 8.01-7.95 (dd, *J* = 7.8, 1.4 Hz, 2H), 7.54-7.47 (m, 1H), 7.45-7.40 (t, *J* = 7.7 Hz, 2H), 6.40-6.36 (s, 1H), 2.27-2.23 (s, 3H); ^{13}C NMR (125 MHz, $CDCl_3$-d_6) δ ppm: 168.30, 155.79, 152.23, 150.78, 134.14, 133.84, 132.02, 128.53, 128.10, 114.07, 103.16, 14.53. HRMS for $C_{14}H_{11}ClN_4O$: *m/z* ([M + H]$^+$): 288.0536, found 288.0524.

***N*-(4-Chloro-6-methyl-7*H*-pyrrolo[2,3-*d*]pyrimidin-2-yl)-4-methoxybenzamide (7b):** Pale yellow solid, yield: 74%, m.p.: 229-230 ºC; ^{1}H NMR (500 MHz, $CDCl_3$-d_6) δ ppm: 10.77-10.73 (s, 1H), 9.68-9.65 (s, 1H), 7.88-7.83 (d, *J* = 8.3 Hz, 2H), 7.01-6.96 (d, *J* = 8.5 Hz, 2H), 6.40-6.36 (s, 1H), 3.77-3.73 (s, 3H), 2.30-2.26 (s, 3H); ^{13}C NMR (125 MHz, $CDCl_3$-d_6) δ ppm: 167.69, 161.75, 154.87, 152.23, 150.78, 133.92, 130.03, 127.68, 115.16, 113.84, 101.08, 55.77, 14.31; HRMS for $C_{15}H_{13}ClN_4O_2$: *m/z* ([M + H]$^+$): 318.0629, found 318.0625.

***N*-(4-Chloro-6-methyl-7*H*-pyrrolo[2,3-*d*]pyrimidin-2-yl)-4-hydroxybenzamide (7c):** Pale yellow solid, yield: 77%, m.p.: 252-253 ºC; ^{1}H NMR (500 MHz, $CDCl_3$-d_6) δ ppm: 10.86-10.83 (s, 1H), 9.77-9.74 (s, 1H), 8.30-8.27 (s, 1H), 7.87-7.82 (d, *J* = 8.8 Hz, 2H), 6.98-6.93 (d, *J* = 8.8 Hz, 2H), 6.52-6.48 (s, 1H), 2.44-2.40 (s, 3H); ^{13}C NMR (125 MHz, $CDCl_3$-d_6) δ ppm: 167.69, 160.22, 155.73, 152.23, 150.78, 134.85, 130.26, 126.60, 117.32, 115.16, 102.52, 14.02; HRMS for $C_{14}H_{11}ClN_4O_2$: *m/z* ([M + H]$^+$) 304.0489, found 304.0486.

***N*-(4-Chloro-6-methyl-7*H*-pyrrolo[2,3-*d*]pyrimidin-2-yl)-3-hydroxybenzamide (7d):** Pale yellow solid, yield: 74%, m.p.: 259-260 ºC; ^{1}H NMR (500 MHz, $CDCl_3$-d_6) δ ppm: 10.54-10.51 (s, 1H), 9.70-9.66 (s, 1H), 8.76-8.72 (s, 1H), 7.59-7.53 (m, 1H), 7.37-7.30 (t, *J* = 8.2 Hz, 1H), 7.30-7.26 (t, *J* = 2.2 Hz, 1H), 6.99-6.93 (dt, *J* = 8.5, 1.6 Hz, 1H), 6.42-6.39 (s, 1H), 2.42-2.39 (s, 3H); ^{13}C NMR (125 MHz, $CDCl_3$-d_6) δ ppm: 129.99, 120.53, 119.65, 114.22, 102.09, 13.67; HRMS for $C_{14}H_{11}ClN_4O_2$: *m/z* ([M + H]$^+$) 304.0512, found 305.0512.

4-Amino-N-(4-chloro-6-methyl-7*H*-pyrrolo[2,3-*d*]-pyrimidin-2-yl)benzamide (7e): Pale yellow solid, yield: 71%, m.p.: 234-235 ºC; ^{1}H NMR (500 MHz, $CDCl_3$-d_6) δ ppm: 10.84-10.80 (s, 1H), 9.63-9.60 (s, 1H), 7.82-7.77 (d, *J* = 8.1 Hz, 2H), 6.62-6.56 (d, *J* = 8.1 Hz, 2H), 6.51-6.47 (s, 1H), 4.51-4.47 (s, 2H), 2.36-2.32 (s, 3H); ^{13}C NMR (125 MHz, $CDCl_3$-d_6) δ ppm: 166.96, 154.87, 153.05, 152.24, 150.78, 133.92, 130.28, 125.19, 115.16, 113.57, 102.09, 13.67; HRMS for $C_{14}H_{12}ClN_5O$: *m/z* ([M + H]$^+$) 303.0865, found 303.0862.

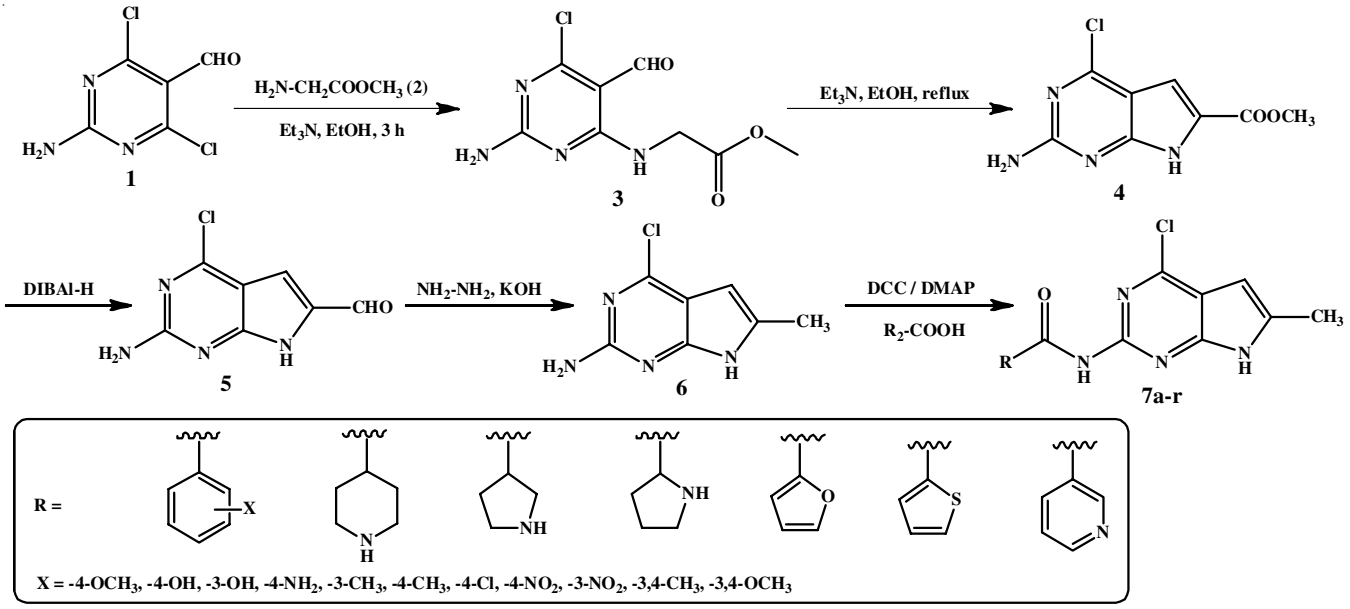

Scheme-I: Synthetic route of the pyrrolo-pyrimidine derivatives (**7a-r**)

***N*-(4-Chloro-6-methyl-7*H*-pyrrolo[2,3-*d*]pyrimidin-2-yl)-3-methylbenzamide (7f):** Pale yellow solid, yield: 80%, m.p.: 228-229ºC; ^{1}H NMR (500 MHz, $CDCl_3$-d_6) δ ppm: 10.65-10.61 (s, 1H), 9.68-9.65 (s, 1H), 7.85-7.78 (dq, *J* = 8.1, 2.0 Hz, 2H), 7.47-7.38 (m, 2H), 6.41-6.37 (s, 1H), 2.39-2.35 (s, 3H), 2.30-2.26 (s, 3H); ^{13}C NMR (125 MHz, $CDCl_3$-d_6) δ ppm: 130.84, 128.73, 128.06, 125.86, 100.79, 20.25, 14.31; HRMS for $C_{15}H_{13}ClN_4O$: *m/z* ([M + H]$^+$) 302.0721, found 302.0717.

***N*-(4-Chloro-6-methyl-7*H*-pyrrolo[2,3-*d*]pyrimidin-2-yl)-4-methylbenzamide (7g):** Pale yellow solid, yield: 75%, m.p.: 223-224ºC; ^{1}H NMR (500 MHz, $CDCl_3$-d_6) δ ppm: 10.83-10.79 (s, 1H), 9.76-9.72 (s, 1H), 7.78-7.73 (d, *J* = 8.1 Hz, 2H), 7.34-7.29 (d, *J* = 8.0 Hz, 2H), 6.38-6.35 (s, 1H), 2.33-2.29 (s, 3H), 2.27-2.23 (s, 3H); ^{13}C NMR (125 MHz, $CDCl_3$-d_6) δ ppm: 166.19, 155.73, 152.23, 149.79, 139.85, 133.92, 130.44, 129.29, 128.38, 114.48, 100.57, 22.21, 14.53; HRMS for $C_{15}H_{13}ClN_4O$ ([M + H]$^+$): 302.0719, found 302.0716.

4-Chloro-*N*-(4-chloro-6-methyl-7*H*-pyrrolo[2,3-*d*]-pyrimidin-2-yl)benzamide (7h): Pale yellow solid, yield: 79%, m.p.: 261-262ºC; ^{1}H NMR (500 MHz, $CDCl_3$-d_6) δ ppm: 10.77-10.73 (s, 1H), 9.67-9.63 (s, 1H), 7.90-7.85 (d, *J* = 8.3 Hz, 2H), 7.55-7.50 (d, *J* = 8.3 Hz, 2H), 6.51-6.47 (s, 1H), 2.39-2.35 (s, 3H); ^{13}C NMR (125 MHz, $CDCl_3$-d_6) δ ppm: 167.71, 156.53, 153.26, 151.31, 137.61, 134.85, 130.87, 129.70, 129.05, 116.73, 103.32, 14.31; HRMS for $C_{14}H_{10}Cl_2N_4O$: *m/z* ([M + H]$^+$) 322.0215, found 322.0213.

***N*-(4-Chloro-6-methyl-7*H*-pyrrolo[2,3-*d*]pyrimidin-2-yl)-4-nitrobenzamide (7i):** Pale yellow solid, yield: 70%, m.p.: 216-217ºC; ^{1}H NMR (500 MHz, $CDCl_3$-d_6) δ ppm: 10.83-10.79 (s, 1H), 9.77-9.74 (s, 1H), 8.29-8.24 (d, *J* = 8.6 Hz, 2H), 8.09-8.04 (d, *J* = 8.6 Hz, 2H), 6.46-6.42 (s, 1H), 2.35-2.31 (s, 3H); ^{13}C NMR (125 MHz, $CDCl_3$-d_6) δ ppm: 165.44, 155.22, 152.23, 150.78, 148.78, 136.73, 133.92, 128.62, 122.96, 113.76, 100.79, 13.30. HRMS for $C_{14}H_{10}ClN_5O_3$: *m/z* ([M + H]$^+$) 333.0476, found 333.0476.

***N*-(4-Chloro-6-methyl-7*H*-pyrrolo[2,3-*d*]pyrimidin-2-yl)-3-nitrobenzamide (7j):** Pale yellow solid, yield: 71%, m.p.: 209-210ºC; ^{1}H NMR (500 MHz, $CDCl_3$-d_6) δ ppm: 10.88-10.84 (s, 1H), 9.77-9.74 (s, 1H), 8.84-8.80 (t, *J* = 2.2 Hz, 1H), 8.48-8.42 (m, 1H), 8.29-8.24 (m, 1H), 7.86-7.79 (t, *J* = 8.5 Hz, 1H), 6.51-6.47 (s, 1H), 2.35-2.31 (s, 3H); ^{13}C NMR (125 MHz, $CDCl_3$-d_6) δ ppm: 133.04, 130.56, 126.15, 123.88, 102.09, 13.67; HRMS for $C_{14}H_{10}ClN_5O_3$: *m/z* ([M + H]$^+$) 333.0476, found 333.0473.

***N*-(4-Chloro-6-methyl-7*H*-pyrrolo[2,3-*d*]pyrimidin-2-yl)-3,4-dimethylbenzamide (7k):** Pale yellow solid, yield: 69%, m.p.: 204-205ºC; ^{1}H NMR (500 MHz, $CDCl_3$-d_6) δ ppm: 10.68-10.64 (s, 1H), 9.62-9.58 (s, 1H), 7.66-7.60 (d, *J* = 7.8 Hz, 2H), 7.17-7.12 (m, 1H), 6.38-6.35 (s, 1H), 2.33-2.29 (s, 3H), 2.28-2.24 (s, 3H), 2.24-2.20 (s, 3H); ^{13}C NMR (125 MHz, $CDCl_3$-d_6) δ ppm: 129.20, 127.89, 126.16, 101.29, 20.76, 19.85, 13.30. HRMS for $C_{16}H_{15}ClN_4O$: *m/z* ([M + H]$^+$) 316.0943, found 316.0941.

***N*-(4-Chloro-6-methyl-7*H*-pyrrolo[2,3-*d*]pyrimidin-2-yl)-3,4-dimethoxybenzamide (7l):** Pale yellow solid, yield: 72%, m.p.: 215-216ºC; ^{1}H NMR (500 MHz, $CDCl_3$-d_6) δ ppm: 10.48-10.44 (s, 1H), 9.65-9.61 (s, 1H), 7.53-7.47 (dd, *J* = 8.5, 2.1 Hz, 1H), 7.44-7.40 (d, *J* = 2.1 Hz, 1H), 7.00-6.95 (d, *J* = 8.5 Hz, 1H), 6.42-6.39 (s, 1H), 3.89-3.86 (s, 3H), 3.85-3.81 (s, 3H), 2.40-2.37 (s, 3H); ^{13}C NMR (125 MHz, $CDCl_3$-d_6) δ ppm: 125.37, 111.64, 110.64, 101.08, 56.58, 55.56, 13.95. HRMS: for $C_{16}H_{15}ClN_4O_3$: *m/z* ([M + H]$^+$) 348.0781, found 348.0779.

***N*-(4-Chloro-6-methyl-7*H*-pyrrolo[2,3-*d*]pyrimidin-2-yl)piperidine-4-carboxamide (7m):** Pale yellow solid, yield: 81%, m.p.: 197-198ºC; ^{1}H NMR (500 MHz, $CDCl_3$-d_6) δ ppm: 9.65-9.61 (s, 1H), 9.34-9.31 (s, 1H), 6.38-6.35 (s, 1H), 3.12-3.05 (s, *J* = 4.0 Hz, 1H), 3.03-2.94 (dddd, *J* = 13.7, 5.5, 3.9, 2.7 Hz, 2H), 2.85-2.76 (dddd, *J* = 13.7, 5.5, 4.0, 2.6 Hz, 2H), 2.72-2.64 (s, *J* = 5.7 Hz, 1H), 2.28-2.24 (s, 3H), 2.12-2.03 (dtd, *J* = 14.0, 5.6, 2.8 Hz, 2H), 1.84-1.76 (dtd, *J* = 14.1, 5.6, 2.7 Hz, 2H); ^{13}C NMR (125 MHz, $CDCl_3$-d_6) δ ppm: 14.02, 27.93, 42.22, 45.15, 102.96, 115.93, 135.22, 149.35, 152.67, 156.45, 174.60; HRMS for $C_{12}H_{16}ClN_5O$: *m/z* ([M + H]$^+$) 295.1023, found 295.1023.

***N*-(4-Chloro-6-methyl-7*H*-pyrrolo[2,3-*d*]pyrimidin-2-yl)pyrrolidine-3-carboxamide (7n):** Pale yellow solid, yield: 74%, m.p.: 189-190ºC; ^{1}H NMR (500 MHz, $CDCl_3$-d_6) δ ppm: 9.72-9.68 (s, 1H), 9.52-9.48 (s, 1H), 6.46-6.42 (s, 1H), 3.20-3.12 (ddd, *J* = 13.3, 4.1, 2.8 Hz, 1H), 3.10-3.02 (m, 1H), 3.02-2.97 (tt, *J* = 4.8, 2.6 Hz, 1H), 2.97-2.90 (m, 1H), 2.90-2.82 (ddd, *J* = 13.3, 4.1, 2.8 Hz, 1H), 2.68-2.62 (m, 1H), 2.37-2.33 (s, 3H), 2.25-2.16 (dtd, *J* = 13.9, 4.2, 2.0 Hz, 1H), 2.10-2.02 (dtd, *J* = 14.0, 4.2, 2.1 Hz, 1H); ^{13}C NMR (125 MHz, $CDCl_3$-d_6) δ ppm: 14.46, 29.75, 43.41, 48.16, 53.52, 102.96, 115.93, 135.43, 151.45, 154.06, 156.16, 174.30; HRMS for $C_{12}H_{14}ClN_5O$: *m/z* ([M + H]$^+$): 281.0888, found 281.0883.

***N*-(4-Chloro-6-methyl-7*H*-pyrrolo[2,3-*d*]pyrimidin-2-yl)pyrrolidine-2-carboxamide (7o):** Pale yellow solid, yield: 71%, m.p.: 184-185ºC; ^{1}H NMR (500 MHz, $CDCl_3$-d_6) δ ppm: 9.76-9.72 (s, 1H), 9.69-9.65 (s, 1H), 6.46-6.42 (s, 1H), 3.93-3.88 (dt, *J* = 5.0, 3.2 Hz, 1H), 3.64-3.58 (dt, *J* = 5.2, 2.6 Hz, 1H), 3.16-3.08 (ddt, *J* = 13.3, 4.7, 2.5 Hz, 1H), 3.03-2.95 (ddt, *J* = 13.3, 4.7, 2.5 Hz, 1H), 2.28-2.24 (s, 3H), 2.17-2.07 (dddd, *J* = 14.2, 7.1, 5.5, 3.2 Hz, 1H), 2.06-1.97 (dddd, *J* = 14.1, 8.6, 5.5, 3.2 Hz, 1H), 1.96-1.77 (m, 2H); ^{13}C NMR (125 MHz, $CDCl_3$-d_6) δ ppm: 13.51, 25.55, 29.74, 47.87, 60.63, 101.58, 114.48, 132.90, 151.24, 153.34, 156.67, 171.97; HRMS for $C_{12}H_{14}ClN_5O$: *m/z* ([M + H]$^+$): 281.0892, found 281.0890.

***N*-(4-Chloro-6-methyl-7*H*-pyrrolo[2,3-*d*]pyrimidin-2-yl)furan-2-carboxamide (7p):** Pale yellow solid, yield: 78%, m.p.: 245-246ºC; ^{1}H NMR (500 MHz, $CDCl_3$-d_6) δ ppm: 9.85-9.82 (s, 1H), 9.67-9.64 (s, 1H), 7.96-7.92 (t, *J* = 1.7 Hz, 1H), 7.34-7.29 (dd, *J* = 5.2, 1.7 Hz, 1H), 6.70-6.65 (dd, *J* = 5.0, 1.6 Hz, 1H), 6.38-6.35 (s, 1H), 2.33-2.29 (s, 3H); ^{13}C NMR (125 MHz, $CDCl_3$-d_6) δ ppm: 14.02, 101.36, 112.72, 115.21, 117.82, 133.55, 146.30, 148.39, 150.68, 152.30, 155.00, 162.04. HRMS for $C_{12}H_9ClN_4O_2$: *m/z* ([M + H]$^+$) 278.0457, found 278.0457.

***N*-(4-Chloro-6-methyl-7*H*-pyrrolo[2,3-*d*]pyrimidin-2-yl)thiophene-2-carboxamide (7q):** Pale yellow solid, yield: 81%, m.p.: 272-273ºC; ^{1}H NMR (500 MHz, $CHCl_3$-d_6) δ ppm: 10.71-10.68 (s, 1H), 9.69-9.65 (s, 1H), 8.12-8.07 (dd, *J* = 5.4, 1.7 Hz, 1H), 7.71-7.66 (dd, *J* = 6.4, 1.6 Hz, 1H), 7.20-7.14 (dd, *J* = 6.4, 5.2 Hz, 1H), 6.54-6.51 (s, 1H), 2.39-2.36 (s, 3H); ^{13}C NMR (125 MHz, $CDCl_3$-d_6) δ ppm: 13.08, 101.58, 114.27, 128.36,

129.89, 132.37, 133.11, 137.83, 150.08, 152.27, 155.95, 165.37; HRMS for $C_{12}H_9ClN_4OS$: *m/z* ([M + H]$^+$): 294.0186, found 294.0181.

***N*-(4-Chloro-6-methyl-7*H*-pyrrolo[2,3-*d*]pyrimidin-2-yl)nicotinamide (7r):** Pale yellow solid, yield: 77%, m.p.: 231-233 ºC; ^{1}H NMR (500 MHz, $CDCl_3$-d_6) δ ppm: 10.89-10.85 (s, 1H), 9.64-9.60 (s, 1H), 9.18-9.14 (t, *J* = 1.8 Hz, 1H), 8.73-8.68 (ddd, *J* = 4.6, 2.7, 1.6 Hz, 1H), 8.25-8.19 (dt, *J* = 8.0, 2.3 Hz, 1H), 7.45-7.39 (dd, *J* = 8.0, 4.8 Hz, 1H), 6.40-6.36 (s, 1H), 2.43-2.39 (s, 3H); ^{13}C NMR (125 MHz, $CDCl_3$-d_6) δ ppm: 14.24, 102.09, 114.48, 123.26, 129.34, 133.92, 136.16, 148.92, 150.54, 151.24, 153.12, 155.73, 166.75. HRMS for $C_{13}H_{10}ClN_5O$: *m/z* ([M + H]$^+$): 289.0473, found 289.0469.

Molecular docking: The Protein Data Bank provided JAK1 (5E1E) and JAK2 (7RN6), CDK 4 (7SJ3) X-ray crystal structures. The Protein Preparation Wizard feature in Schrödinger software added hydrogen atoms and allocated bond orders in the 3D structure of protein. The LigPrep module in Schrödinger software prepared chiral ligands and optimized their 3D structures using the OPLS 2005 force field software. The SITEMAP ANALYSIS TOOL of Maestro 11.8 was used to analyze receptor sites for 5E1E, 7RN6 and 7SJ3 followed by Schrödinger suite's grid creation tool. The SP Glide score was derived using binding interaction energy, van der Waals energy, electrostatic potential energy and strain energy assessments during the molecular docking using Glide's standard precision docking modes (Glide XP). The Schrödinger Maestro interface was used to study ligand binding to EGFR and CDK-4 active sites [31].

MTT assay: To evaluate the anticancer activity of pyrrolo-pyrimidine derivatives (**7a-r**), an MTT assay was conducted using the HCT-116 (colon cancer), MCF-7 (breast cancer), SET-2 (chronic myeloid leukemia) and HEK-293 (normal human embryonic kidney) cell lines. The cell lines were cultured in RPMI-1640 or DMEM medium, supplemented with 10% fetal bovine serum (FBS) and 1% penicillin-streptomycin, at 37 ºC in a 5% CO_2 incubator. Upon reaching 70-80% confluence, the adherent cells (MCF-7, HCT-116 and HEK-293) were trypsinized using trypsin-EDTA, while SET-2 cells were gently suspended by pipetting. Approximately 5,000-10,000 cells per well were seeded in 100 µL of complete medium in 96-well plates and allowed to attach and stabilize for 24 h.

Serial dilutions of the synthesized derivatives (**5a-r**) were prepared in complete medium to achieve concentrations ranging from 0.1 µM to 100 µM. The medium in each well was replaced with 100 µL of these compound dilutions, with a control group treated with an equivalent volume of DMSO (vehicle control). The plates were incubated for 48 h. Following treatment, 10 µL of MTT reagent (5 mg/mL in PBS) was added to each well and the plates were incubated for an additional 4 h at 37 ºC to allow for the formation of formazan crystals. The medium containing the MTT reagent was then carefully removed and 100 µL of DMSO was added to each well to dissolve the formazan crystals. The plates were gently shaken for 10-15 min to ensure the complete dissolution.

The absorbance was measured at 570 nm using a microplate reader, with a reference wavelength of 630 nm to correct for background absorbance. The IC_{50} values, representing the concentration of compound required to inhibit cell growth by 50%, were determined for each derivative by plotting cell viability against the concentration. All the procedures were performed under sterile conditions to prevent contamination and multiple replicates (n = 3) were included for each concentration to ensure data reliability [32].

RESULTS AND DISCUSSION

The synthesis of the title compounds initiated with 2-amino-4,6-dichloropyrimidine-5-carbaldehyde (**1**), which undergoes a reaction with methyl glycinate (**2**) in the presence of ethanol and triethylamine at room temperature, yielding the ester intermediate methyl (2-amino-6-chloro-5-formylpyrimidin-4-yl)-glycinate (**3**).

Prolonged heating of intermediate **3** in ethanol with triethylamine induces a cyclization reaction, forming methyl 2-amino-4-chloro-7*H*-pyrrolo[2,3-*d*]pyrimidine-6-carboxylate (**4**). The methyl ester **4** was then selectively reduced to the aldehydic intermediate, 2-amino-4-chloro-7*H*-pyrrolo[2,3-*d*]pyrimidine-6-carbaldehyde (**5**), using DIBAL-H under controlled conditions at -78 ºC. Subsequently, the aldehyde group in compound **5** is reduced to a methyl group *via* the Wolff-Kishner reduction, employing hydrazine and KOH, resulting in 4-chloro-6-methyl-7*H*-pyrrolo[2,3-*d*]pyrimidin-2-amine (**6**). In the final step, compound **6** was condensed with various substituted aryl/heteroaryl carboxylic acids in a coupling reaction facilitated by DCC and DMAP, producing a series of amide-linked pyrrolo[2,3-*d*]-pyrimidine derivatives (**7a-r**).

All synthesized compounds were obtained in moderate to good yields, ranging from 69% to 81%. In the proton NMR spectra, the major N-H peak of the pyrrole ring, indicative of cyclization, appeared as a singlet in the region of 9.5 to 9.8 ppm. Another significant N-H peak, corresponding to the formation of the amide bond between the R-COOH group and the amine of the pyrrolo[2,3-*d*]pyrimidine ring, was observed in the region of 10.6 to 10.9 ppm. All aromatic protons exhibited peaks in the respective regions between 6.0 to 8.0 ppm. In the ^{13}C NMR spectra, the carbonyl carbon peaks of the final compounds appeared in the region of 160 to 175 ppm. The carbon of the pyrrole ring were observed around 100 to 110 ppm, while the carbons bonded to nitrogen were detected in the range of 130 to 140 ppm. The HRMS confirmed the molecular weight of the final compounds, with all synthesized compounds producing the respective $(M+H)^+$ peaks, consistent with the expected molecular masses.

Molecular docking studies: The docking investigations of synthesized pyrrolo-pyrimidine derivatives (**7a-r**) against three specific target molecules *viz*. JAK1 kinase (5E1E), JAK2 kinase domain (7RN6) and CDK4 (7SJ3) have provided valuable insights into their binding affinities and possible therapeutic effectiveness. The docking scores, which represent the binding free energy, suggest significant interactions, with greater negative values indicating superior binding. The docking scores of the designed derivative are listed in Table-1.

For the JAK1 kinase target, the docking scores of the derivatives range from -5.675 to -6.915. Among these, compound

TABLE-1
DOCKING SCORES OF DESIGNED PYRROLO-PYRIMIDINE DERIVATIVES (**7a-r**)

Compound	R-group	Docking score		
		JAK1 Kinase (5E1E)	JAK2 Kinase domain (7RN6)	CDK4 (7SJ3)
7a	Benzene	-6.44	-8.267	-6.464
7b	4-Methoxy benzene	-5.717	-8.702	-6.33
7c	4-Hydroxy benzene	-6.401	-8.362	-6.328
7d	3-Hydroxy benzene	-6.435	-8.258	-7.306
7e	4-Amino benzene	-5.708	-8.347	-5.884
7f	3-Methyl benzene	-6.72	-8.624	-6.74
7g	4-Methyl benzene	-6.68	-8.762	-6.657
7h	4-Chloro benzene	-5.675	-8.469	-6.703
7i	4-Nitro benzene	-6.103	-7.379	-6.058
7j	3-Nitro benzene	-6.233	-8.468	-7.079
7k	3,4-Dimethyl benzene	-6.915	-8.914	-6.876
7l	3,4-Dimethoxy benzene	-6.05	-8.94	-6.338
7m	Piperidine	-6.468	-7.371	-6.058
7n	Pyrrolidine	-6.33	-7.561	-6.564
7o	Proline	-6.485	-7.455	-6.934
7p	Furan	-6.008	-7.577	-5.657
7q	Thiophene	-6.2	-7.958	-5.519
7r	Pyridine	-5.684	-8.091	-5.895
5E1E Ligand	–	-11.301	–	–
7RN6 Ligand	–	–	-10.643	–
7SJ3 Ligand	–	–	–	-7.541
Doxorubicin	–	-8.969	-7.238	-8.434

7k (3,4-dimethyl benzene) stands out with the highest binding affinity, scoring -6.915, closely followed by compound **7f** (3-methyl benzene) at -6.72 (Fig. 2) and compound **7g** (4-methyl benzoic acid) at -6.68. These compounds show substantial potential for binding to JAK1 kinase. While compounds like **7h** (4-chloro benzene), **7b** (4-methoxy benzene) and **7r** (pyridine) have slightly lower affinities, they still exhibit notable binding capabilities. The reference ligand for JAK1 kinase demonstrates a strong binding affinity with a score of -11.301, setting a high benchmark that some derivatives come close to achieving.

In case of the JAK2 kinase domain, the docking scores span from -7.371 to -8.94. Compound **7l** (3,4-dimethoxy benzene) exhibits the highest binding affinity with a score of -8.94, followed closely by compound **7k** (3,4-dimethyl benzene) at -8.914 (Fig. 3) and compound **7g** (4-methyl benzene) at -8.762. These results highlighted the strong binding potential

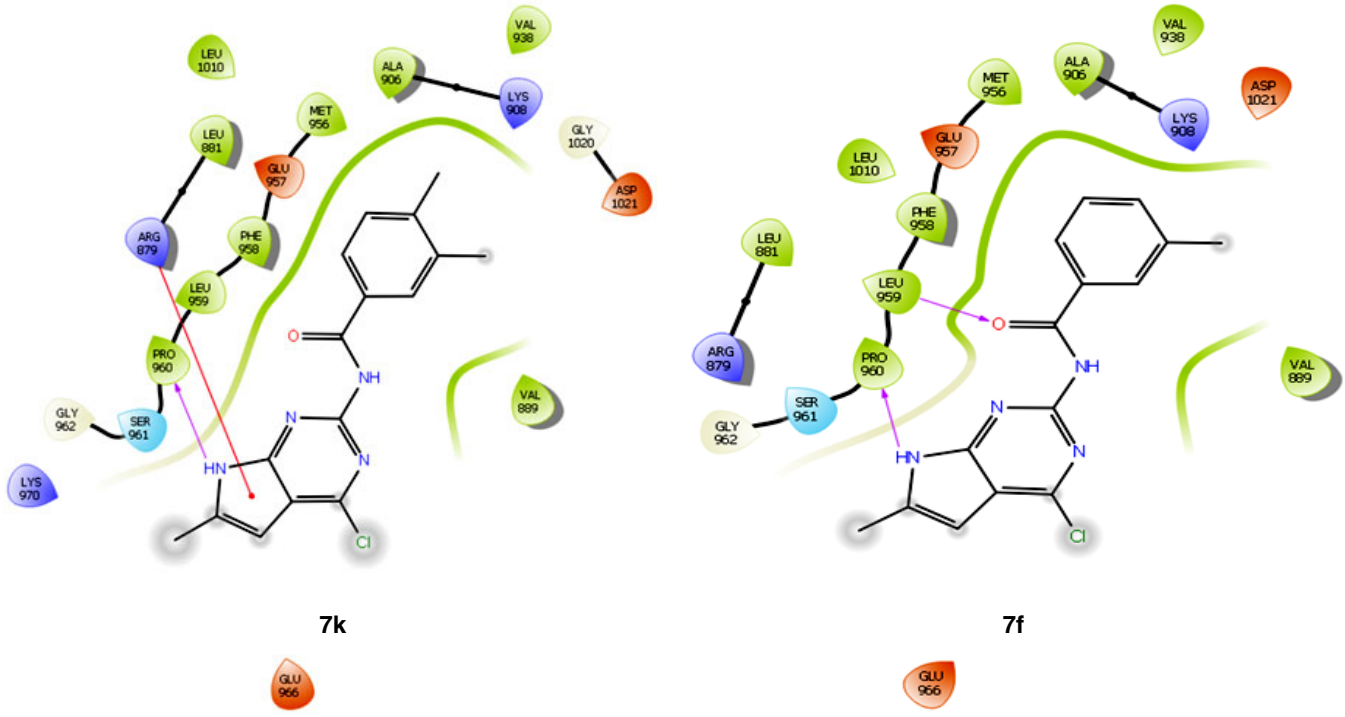

Fig. 2. Interactions of compounds **7k** and **7f** at the active site of JAK1

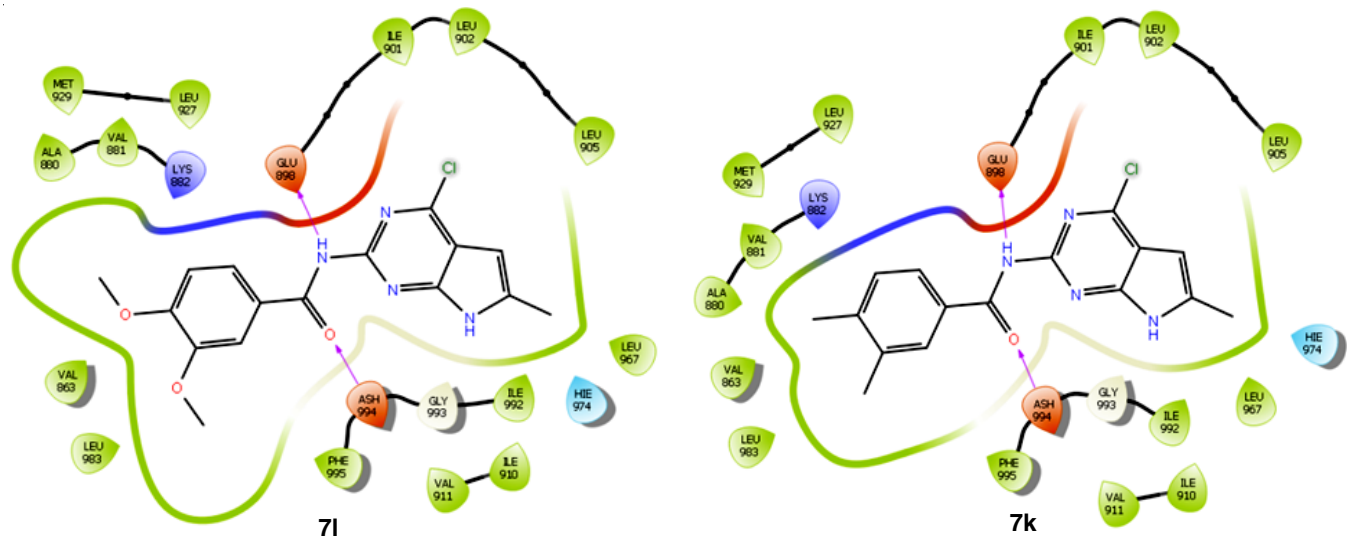

Fig. 3. Interactions of compounds **7l** and **7k** at the active site of JAK2

of these derivatives with JAK2 kinase domain. Even the lower-scoring compounds, such as compounds **7i** (4-nitro benzene) and **7m** (piperidine), still show significant binding with scores of -7.379 and -7.371, respectively. The reference ligand for JAK2 kinase domain shows a binding affinity score of -10.643, with several derivatives demonstrating close affinity, exhibiting their therapeutic potential.

For CDK4 target, the docking scores range from -5.519 to -7.306. Compound **7d** (3-hydroxy benzene) displays the highest binding affinity with a score of -7.306, followed by compound **7j** (3-nitro benzene) at -7.079 (Fig. 4) and compound **7o** (proline) at -6.934. These compounds exhibit considerable potential for binding to CDK4. Even the compounds with lower scores, such as compounds **7q** (thiophene) and **7p** (furan), still demonstrate meaningful binding affinities with scores of -5.519 and -5.657, respectively. The reference ligand for CDK4 shows a binding affinity of -7.541 and several derivatives approach this high affinity, indicating their potential for optimization.

Doxorubicin, used as a control in these studies, shows high binding affinities across all targets: -8.969 for JAK1 kinase, -7.238 for JAK2 kinase domain and -8.434 for CDK4. This comparison highlights that the pyrrolo-pyrimidine derivatives are competitive, with many showing strong binding affinities that approach those of doxorubicin, especially with JAK1 kinase and CDK4.

Pyrrolo-pyrimidine derivatives (**7a-r**) exhibit a range of strong binding affinities across the three target molecules. Compounds **7k** (3,4-dimethyl benzene) and **7l** (3,4-dimethoxy benzene) consistently demonstrate impressive binding, particularly with JAK2 kinase domain. A significant portion of the derivatives have binding affinities that are nearly equivalent to those of the reference ligands, suggesting significant potential for further optimization. These docking studies offer valuable insights that can be used to guide the development of derivatives with even more potent properties and improved binding characteristics, thereby facilitating the development of novel therapeutic agents that target these kinases.

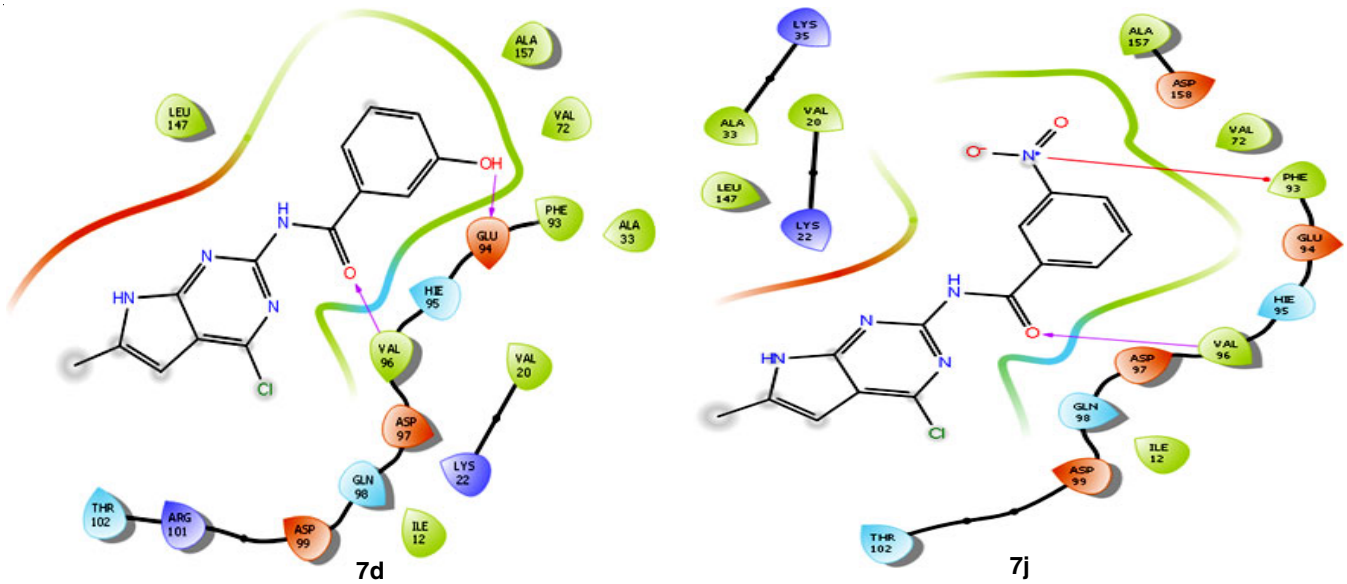

Fig. 4. Interactions of compounds **7** and **7j** at the active site of JAK2

Anticancer activity: The results of the cytotoxicity studies of the synthesized pyrrolo-pyrimidine derivative (**7a-r**) against the selected cell lines were enumerated in terms of IC_{50} and selectivity index in Table-2. Human Embryonic Kidney (HEK-293) cells were utilized in this investigation to evaluate the cytotoxic effects of synthesized compounds on normal cells. The IC_{50} values of these compounds were used to calculate selectivity indices across all tested cancer cell lines.

Breast cancer cells (MCF-7): The MTT assay results highlight the potential of compounds **7a-r** as anticancer agents against MCF-7 breast cancer cells. Among the derivatives tested, several demonstrated significant cytotoxicity, with some showing efficacy comparable to that of the standard chemotherapy drug doxorubicin (IC_{50} = 2.39 ± 0.75 μM). The IC_{50} values for the compounds range from 5.66 μM to 18.5 μM.

The most potent compounds are compound **7k** (3,4-dimethyl benzene) with an IC_{50} of 5.66 μM, compound **7f** (3-methyl benzene) with an IC_{50} of 5.78 μM, compound **7g** (4-methyl benzoic acid) with an IC_{50} of 8.12 μM and **7o** (proline) with an IC_{50} of 8.95 μM. These compounds show the highest potency among the tested derivatives, suggesting that methyl substitutions on the benzene ring and the presence of the proline ring enhance anticancer activity. Moderately potent compounds include compound **7c** (4-hydroxy benzene) with an IC_{50} of 10.03 μM, compound **7d** (3-hydroxy benzene) with an IC_{50} of 12.0 μM, compound **7m** (piperidine) with an IC_{50} of 10.97 μM and compound **7n** (pyrrolidine) with an IC_{50} of 11.38 μM. These compounds also exhibit significant potency, indicating that the presence of hydroxyl groups and cyclic amines can contribute positively to anticancer activity. The least potent compounds are **7l** (3,4-dimethoxy benzene) with an IC_{50} of 18.5 μM, **7i** (4-nitro benzene) with an IC_{50} of 18.29 μM, **7h** (4-chloro benzene) with an IC_{50} of 16.39 μM and **7q** (thiophene) with an IC_{50} of 15.68 μM. The compounds with nitro, chloro and methoxy substitutions are less potent, suggesting that these groups might not favour the interaction with the cancer cells as effectively as other substituents.

A higher value for the selectivity index indicates that the substance is more selective in its targeting of cancer cells compared to normal cells. The SI values for the compounds range from 1.52 to 5.55, while doxorubicin, the reference standard, has an SI of 2.02. The most selective compounds are **7k** (3,4-dimethyl benzene) with an SI of 5.55, **7f** (3-methyl benzene) with an SI of 5.2 and **7g** (4-methyl benzene) with an SI of 3.68. These high SI values suggest that these compounds are more selective for MCF-7 cancer cells, likely due to the methyl substitutions.

Moderately selective compounds include **7c** (4-hydroxy benzene) with an SI of 3.09, **7o** (proline) with an SI of 3.1, **7n** (pyrrolidine) with an SI of 2.85 and **7j** (3-nitro benzene) with an SI of 2.67. These compounds show good selectivity, benefiting from hydroxyl, proline and pyrrolidine groups. The least selective compounds are **7l** (3,4-dimethoxy benzene) with an SI of 1.52, **7e** (4-amino benzene) with an SI of 1.77, **7h** (4-chloro benzene) with an SI of 1.95, **7i** (4-nitro benzene) with an SI of 1.92 and **7q** (thiophene) with an SI of 1.9. These low SI values suggest less favourable selectivity for cancer cells.

Certain pyrrolo-pyrimidine derivatives, particularly those with methyl, hydroxyl, proline and pyrrolidine groups, exhibit higher selectivity indices than doxorubicin, indicating potential as more selective anticancer agents. Conversely, compounds with methoxy, amino, chloro, nitro and thiophene groups show lower selectivity, indicating a need for further optimization.

Chronic myeloid leukemia cells (SET-2): The IC_{50} values of pyrrolo pyrimidine derivatives (**7a-r**) against SET-2 cells range from 8.61 ± 1.02 to 18.79 ± 0.92 μM. Doxorubicin, the standard drug, has an IC_{50} value of 3.54 ± 0.56 μM. Among

TABLE-2
THE MTT ASSAY DATA OF PYRROLO-PYRIMIDINE DERIVATIVES (**7a-r**)

Compound	IC_{50} (μM)				Selectivity Index		
	Breast cancer (MCF-7)	Chronic myeloid leukemia (SET-2)	Colon cancer (HCT-116)	Human embryonic kidney cell (HEK-293)	Breast cancer (MCF-7)	Chronic myeloid leukemia (SET-2)	Colon cancer (HCT-116)
7a	15.16 ± 0.97	16.26 ± 1.77	10.91 ± 1.44	35.32 ± 0.97	2.33	2.17	3.24
7b	15.44 ± 2.24	13.65 ± 1.53	12.90 ± 2.55	32.67 ± 1.47	2.12	2.40	2.53
7c	10.03 ± 0.79	11.54 ± 1.11	14.62 ± 1.59	31.02 ± 4.11	3.09	2.69	2.12
7d	12.0 ± 1.82	13.58 ± 1.10	16.25 ± 0.92	29.50 ± 1.83	2.46	2.17	1.82
7e	14.38 ± 1.26	13.78 ± 1.28	19.05 ± 1.28	25.48 ± 4.11	1.77	1.85	1.34
7f	5.78 ± 0.91	9.23 ± 1.81	9.20 ± 0.97	30.06 ± 2.22	5.20	3.26	3.27
7g	8.12 ± 0.96	12.12 ± 1.02	7.50 ± 2.33	29.84 ± 1.14	3.68	2.46	3.98
7h	16.39 ± 2.91	13.58 ± 1.10	9.88 ± 0.91	31.99 ± 1.03	1.95	2.36	3.24
7i	18.29 ± 1.96	12.90 ± 3.49	13.14 ± 1.77	35.05 ± 1.43	1.92	2.72	2.67
7j	13.26 ± 0.97	13.41 ± 1.77	12.97 ± 1.76	35.32 ± 0.83	2.67	2.63	2.72
7k	5.66 ± 0.97	9.92 ± 2.75	6.04 ± 1.22	31.38 ± 1.43	5.55	3.16	5.19
7l	18.5 ± 0.96	15.44 ± 1.02	6.72 ± 1.44	28.01 ± 2.93	1.52	1.81	4.17
7m	10.33 ± 0.9	8.61 ± 1.02	18.71 ± 2.33	24.97 ± 2.77	2.42	2.90	1.33
7n	11.38 ± 1.77	10.33 ± 1.48	13.77 ± 2.26	32.42 ± 1.20	2.85	3.14	2.35
7o	8.95 ± 0.96	9.44 ± 1.53	16.01 ± 1.11	27.67 ± 1.20	3.10	2.93	1.73
7p	14.72 ± 1.28	16.52 ± 1.59	15.30 ± 0.92	30.06 ± 2.22	2.04	1.82	1.96
7q	15.68 ± 1.61	18.15 ± 1.87	14.38 ± 1.26	29.84 ± 1.14	1.90	1.64	2.08
7r	15.28 ± 0.91	18.79 ± 0.92	15.25 ± 1.77	31.99 ± 1.03	2.09	1.70	2.10
Doxorubicin	2.39 ± 0.75	3.54 ± 0.56	3.10 ± 0.81	4.83 ± 1.12	2.02	1.36	1.55

the most potent compounds are **7k** (3,4-dimethyl benzene), **7f** (3-methyl benzene) and **7m** (piperidine), which exhibited IC_{50} values ranging from 8.61 ± 1.02 to 9.92 ± 2.75 μM. These compounds demonstrate strong cytotoxic effects, requiring lower concentrations to inhibit 50% of cell growth compared to others tested. In the moderately potent category, compounds like **7g** (4-methyl benzene), **7i** (4-nitro benzene) and **7h** (4-chloro benzene) showed IC_{50} values between 12.12 ± 1.02 and 13.58 ± 3.49 μM, indicating effective inhibition but not as potent as the top-tier compounds. Conversely, the least potent compounds included **7r** (pyridine), **7q** (thiophene) and **7p** (furan), with IC_{50} values ranging from 16.52 ± 1.59 to 18.79 ± 0.92 μM, suggesting they have weaker cytotoxic effects.

The SI values of synthesized pyrrolo-pyrimidine derivatives (**7a-r**) ranging from 1.64 to 3.26 indicate varying degrees of selectivity for cancer cells over normal cells. Compounds with SI values above 2, such as **7f** (3-methyl benzene), **7k** (3,4-dimethyl benzene), **7l** (3,4-dimethoxy benzene), **7n** (pyrrolidine) and **7o** (proline), demonstrate promising selectivity profiles. These compounds exhibit both low IC_{50} values, indicating potent cytotoxic effects against cancer cells and high SI values, suggesting reduced toxicity to normal cells.

The impact of benzene ring substituents on the cytotoxicity of pyrrolo-pyrimidine derivatives against chronic myeloid leukemia cells is emphasized by the structure-activity relationship (SAR) study. Compounds with these substitutions show variable IC_{50} values, indicating their potency is strongly influenced by the type and position of substituents. In contrast, derivatives containing heterocyclic rings like furan (**7p**), thiophene (**7q**) and pyridine (**7r**) generally exhibit higher IC_{50} values than benzene derivatives, suggesting potentially lower cytotoxicity in this assay. Compounds such as **7f**, **7k**, **7l**, **7n** and **7o** emerge as notable candidates due to their favourable combination of potent cytotoxicity and high selectivity.

Colon cancer cells (HCT-116): The assessment of pyrrolo-pyrimidine derivatives (**7a-r**) against colon cancer cells (HCT-116) has unveiled a spectrum of cytotoxic profiles and selectivity indices (SI). Doxorubicin, utilized as the standard, demonstrated an IC_{50} value of 3.10 ± 0.81 μM. Among the derivatives, those displaying the lowest IC_{50} values were identified as the most potent in inhibiting cell growth. Specifically, compounds such as **7k** (3,4-dimethyl benzene), **7l** (3,4-dimethoxy benzene), **7g** (4-methyl benzene) and **7f** (3-methyl benzene) exhibited IC_{50} values ranging from 6.04 ± 1.22 to 9.20 ± 0.97 μM. Moderately potent compounds, including **7h** (4-chloro benzene), **7a** (benzene), **7i** (4-nitro benzene) and **7j** (3-nitro benzene), demonstrated intermediate efficacy with IC_{50} values ranging from 9.88 ± 0.91 to 13.14 ± 1.77 μM. Conversely, compounds with higher IC_{50} values, such as **7e** (4-amino benzene), **7m** (piperidine), **7n** (pyrrolidine), **7o** (proline), **7p** (furan), **7q** (thiophene) and **7r** (pyridine), were identified as the least potent, indicating diminished efficacy in inhibiting colon cancer cell growth under the tested conditions, with IC_{50} values ranging from 13.77 ± 2.26 to 19.05 ± 1.28 μM.

The SI values of these compounds ranged from 1.33 to 5.19, underscoring their varying degrees of selectivity for cancerous cells over normal ones. Compounds **7k**, **7l**, **7g** and **7f** exhibited noteworthy SI values ranging from 3.27 to 5.19, suggesting significant cytotoxic effects against HCT-116 cells while demonstrating relative sparing of normal cells. Structural analysis (SAR) highlighted the critical role of substituents in modulating potency against colon cancer cells, with methyl substitutions in compounds like **7g**, **7f**, **7k** and **7l** correlating with lower IC_{50} values and heightened efficacy in inhibiting cancer cell growth. Furthermore, the presence of electron-donating or withdrawing groups such as methyl, methoxy, hydroxy and nitro influenced both potency and selectivity profiles across these derivatives.

In contrast, heterocyclic compounds exhibited distinct cytotoxic profiles against HCT-116 cells. Derivatives like **7m** (piperidine), **7n** (pyrrolidine), **7o** (proline), **7p** (furan), **7q** (thiophene) and **7r** (pyridine) generally demonstrated moderate to high IC_{50} values, indicating varying degrees of potency compared to their benzene counterparts. Their SI values suggested potential differences in mechanisms of action, implicating complex interactions within cancer cells. These findings underscore the intricate relationship between chemical structure, cytotoxic efficacy and selectivity in the development of pyrrolo-pyrimidine derivatives as potential therapies for colon cancer.

The correlation between the anticancer activity of pyrrolo-pyrimidine derivatives (**7a-r**) and their molecular docking results reveals compelling insights into their therapeutic potential. In breast cancer cell line MCF-7, compounds like **7k** (3,4-dimethyl benzene), **7f** (3-methyl benzene) and **7g** (4-methyl benzoic acid) demonstrate potent cytotoxicity with IC_{50} values ranging from 5.66 μM to 8.12 μM. These results align closely with their strong binding affinities observed in molecular docking studies, where compounds such as compound **7k** exhibit high scores against JAK1 kinase (-6.915). This correlation suggests that the potent cytotoxic effects observed in MCF-7 cells may be attributed to their effective inhibition of JAK1 kinase, highlighting a potential therapeutic mechanism. Similarly, in chronic myeloid leukemia cell line SET-2, compounds **7k**, **7f** and **7m** (piperidine) display significant cytotoxicity with IC_{50} values between 8.61 μM and 9.92 μM, paralleled by strong binding affinities to targets such as JAK2 kinase domain (*e.g.* **7k** with a docking score of -8.914). This suggests that inhibition of JAK2 kinase could contribute to their efficacy against chronic myeloid leukemia. In colon cancer cell line HCT-116, compounds **7k**, **7l**, **7g** and **7f** exhibit potent cytotoxicity (IC_{50} values from 6.04 μM to 9.20 μM) and demonstrate robust binding interactions with targets like JAK2 kinase domain (-8.94 for **7l**). This correlation underscores the role of specific kinase inhibition, including CDK4, in mediating their anticancer activity. Overall, the strong alignment between cytotoxic potency and binding affinities across different cancer cell lines underscores the promise of pyrrolo-pyrimidine derivatives as targeted therapeutic agents, guided by their specific interactions with key oncogenic proteins identified through molecular docking studies.

Conclusion

Through a systematic synthesis approach, diverse pyrrolo-pyrimidine derivatives (**7a-r**) were successfully prepared and

characterized. Computational docking studies against JAK1, JAK2 and CDK4 revealed promising binding affinities, suggesting their efficacy against these key kinase targets implicated in cancer. *In vitro* MTT assays across MCF-7, SET-2 and HCT-116 cell lines demonstrated varied but potent cytotoxicity profiles for several derivatives. Compounds **7k**, **7f** and **7g** showed significant activity against MCF-7 and SET-2 cells, while **7k**, **7l**, **7g** and **7f** exhibited strong effects against HCT-116 cells. Moreover, high selectivity indices against cancer cells compared to normal HEK-293 cells underscored their potential as selective anticancer agents. The structure-activity relationship (SAR) analysis highlighted the impact of specific substituents, such as methyl and hydroxyl groups, on enhancing cytotoxic potency. The findings of this position in this pyrrolo-pyrimidine derivatives (**7a-r**) as promising candidates for further development as potential anticancer agents.

ACKNOWLEDGEMENTS

The authors are grateful for the support provided by the Andhra University, Visakhapatnam which was instrumental in the successful completion of this research work.

CONFLICT OF INTEREST

The authors declare that there is no conflict of interests regarding the publication of this article.

REFERENCES

1. World Health Organization, Global Cancer Burden Growing, Amidst Mounting Need for Services (2024); https://www.who.int/news/item/01-02-2024-global-cancer-burden-growing--amidst-mounting-need-for-services
2. R. Baskar, K.A. Lee, R. Yeo and K.W. Yeoh, *Int. J. Med. Sci.*, **9**, 193 (2012); https://doi.org/10.7150/ijms.3635
3. D.T. Debela, S.G. Muzazu, K.D. Heraro, M.T. Ndalama, B.W. Mesele, D.C. Haile, S.K. Kitui and T. Manyazewal, *SAGE Open Med.*, **9**, 20503121211034366 (2021); https://doi.org/10.1177/20503121211034366
4. U. Anand, A. Dey, A.K.S. Chandel, R. Sanyal, A. Mishra, D.K. Pandey, V. De Falco, A. Upadhyay, R. Kandimalla, A. Chaudhary, J.K. Dhanjal, S. Dewanjee, J. Vallamkondu and J.M. Pérez de la Lastra, *Genes Dis.*, **10**, 1367 (2023); https://doi.org/10.1016/j.gendis.2022.02.007
5. I.A. George, R. Chauhan, R. Dhawale, R. Iyer, S. Limaye, R. Sankaranarayanan, R. Venkataramanan and P. Kumar, *Adv. Cancer Biol. Metastasis*, **6**, 100074 (2022); https://doi.org/10.1016/j.adcanc.2022.100074
6. S.L. Groenland, A. Martínez-Chávez, M.G.J. van Dongen, J.H. Beijnen, A.H. Schinkel, A.D.R. Huitema and N. Steeghs, *Clin. Pharmacokinet.*, **59**, 1501 (2020); https://doi.org/10.1007/s40262-020-00930-x
7. T.Y.J. Appeldoorn, T.H.O. Munnink, L.M. Morsink, M.N.L.D. Hooge and D.J. Touw, *Clin. Pharmacokinet.*, **62**, 559 (2023); https://doi.org/10.1007/s40262-023-01225-7
8. V. Beljanski, *Compr. Pharmacol. Ref.*, **1**, 1 (2007); https://doi.org/10.1016/B978-008055232-3.63731-6
9. X. Liang, S. Tang, X. Liu, Y. Liu, Q. Xu, X. Wang, A. Saidahmatov, C. Li, J. Wang, Y. Zhou, Y. Zhang, M. Geng, M. Huang and H. Liu, *J. Med. Chem.*, **65**, 1243 (2022); https://doi.org/10.1021/acs.jmedchem.0c02111
10. J. Zhang, S. Xing, J. Cui, X. Wei, Z. Cao, B. Shao, N. Jiang and X. Zhai, *Arch. Pharm.*, **357**, 2300591 (2024); https://doi.org/10.1002/ardp.202300591
11. W. Mao, H. Wu, Q. Guo, X. Zheng, C. Wei, Y. Liao, L. Shen, J. Mi, J. Li, S. Chen and W. Qian, *Bioorg. Med. Chem. Lett.*, **74**, 128905 (2022); https://doi.org/10.1016/j.bmcl.2022.128905
12. B. Yang, Y. Quan, W. Zhao, Y. Ji, X. Yang, J. Li, Y. Li, X. Liu, Y. Wang and Y. Li, *J. Enzyme Inhib. Med. Chem.*, **38**, 2169282 (2023); https://doi.org/10.1080/14756366.2023.2169282
13. S.M. Patil, V.A. Patil, K. Asgonkar, V. Randive and I. Mahadik, *Curr. Indian Sci.*, **01**, e2210299X258569 (2023); https://doi.org/10.2174/012210299X258569231006094309
14. X. Shi, Y. Quan, Y. Wang, Y. Wang and Y. Li, *Bioorg. Med. Chem. Lett.*, **33**, 127725 (2021); https://doi.org/10.1016/j.bmcl.2020.127725
15. Y. Li, R. Du, Y. Nie, T. Wang, Y. Ma and Y. Fan, *Bioorg. Chem.*, **109**, 104717 (2021); https://doi.org/10.1016/j.bioorg.2021.104717
16. L.X. Wang, X. Liu, S. Xu, Q. Tang, Y. Duan, Z. Xiao, J. Zhi, L. Jiang, P. Zheng and W. Zhu, *Eur. J. Med. Chem.*, **141**, 538 (2017); https://doi.org/10.1016/j.ejmech.2017.10.027
17. P. Shirvani and A. Fassihi, *Mol. Simul.*, **46**, 1265 (2020); https://doi.org/10.1080/08927022.2020.1810853
18. D. Xu, D. Sun, W. Wang, X. Peng, Z. Zhan, Y. Ji, Y. Shen, M. Geng, J. Ai and W. Duan, *Eur. J. Med. Chem.*, **220**, 113497 (2021); https://doi.org/10.1016/j.ejmech.2021.113497
19. X. Zhao, W. Huang, Y. Wang, M. Xin, Q. Jin, J. Cai, F. Tang, Y. Zhao and H. Xiang, *Bioorg. Med. Chem.*, **23**, 891 (2015); https://doi.org/10.1016/j.bmc.2014.10.043
20. L. He, H. Pei, C. Zhang, M. Shao, D. Li, M. Tang, T. Wang, X. Chen, M. Xiang and L. Chen, *Eur. J. Med. Chem.*, **145**, 96 (2018); https://doi.org/10.1016/j.ejmech.2017.12.079
21. Z. Xia, R. Huang, X. Zhou, Y. Chai, H. Chen, L. Ma, Q. Yu, Y. Li, W. Li and Y. He, *Eur. J. Med. Chem.*, **224**, 113711 (2021); https://doi.org/10.1016/j.ejmech.2021.113711
22. S.J. Kaspersen, J. Han, K.G. Nørsett, L. Rydså, E. Kjøbli, S. Bugge, G. Bjørkøy, E. Sundby and B.H. Hoff, *Eur. J. Pharm. Sci.*, **59**, 69 (2014); https://doi.org/10.1016/j.ejps.2014.04.011
23. G. Sivaiah, R. Raveesha, S. Benaka Prasad, K. Yogesh Kumar, M. Raghu, F.A. Alharti, M. Prashanth and B.H. Jeon, *J. Mol. Struct.*, **1275**, 134728 (2023); https://doi.org/10.1016/j.molstruc.2022.134728
24. A.A. Alotaibi, M.M. Alanazi and A.F.M.M. Rahman, *Pharmaceuticals*, **16**, 1324 (2023); https://doi.org/10.3390/ph16091324
25. K. Metwally and N.E. Abo-Dya, *Curr. Med. Chem.*, **31**, 5918 (2024); https://doi.org/10.2174/0929867331666230815115111
26. M. Adel, R.A. Serya, D.S. Lasheen and K.A. Abouzid, *Bioorg. Chem.*, **81**, 612 (2018); https://doi.org/10.1016/j.bioorg.2018.09.001
27. A.A. Alotaibi, H.H. Asiri, A.M. Rahman and M.M. Alanazi, *J. Saudi Chem. Soc.*, **27**, 101712 (2023); https://doi.org/10.1016/j.jscs.2023.101712
28. S. Tumkevicius, M. Dailide and A. Kaminskas, *J. Heterocycl. Chem.*, **43**, 1629 (2006); https://doi.org/10.1002/jhet.5570430630
29. L. Ducry and D.M. Roberge, *Org. Process Res. Dev.*, **12**, 163 (2008); https://doi.org/10.1021/op7002002
30. D. Webb and T.F. Jamison, *Org. Lett.*, **14**, 568 (2012); https://doi.org/10.1021/ol2031872
31. B.J. Bender, S. Gahbauer, A. Luttens, J. Lyu, C.M. Webb, R.M. Stein, E.A. Fink, T.E. Balius, J. Carlsson, J.J. Irwin and B.K. Shoichet, *Nat. Protoc.*, **16**, 4799 (2021); https://doi.org/10.1038/s41596-021-00597-z
32. T.L. Riss, R.A. Moravec, A.L. Niles, S. Duellman, H.A. Benink, T.J. Worzella and L. Minor, Assay Guidance Manual, Eli Lilly & Company and the National Center for Advancing Translational Sciences (2016).